Description of Scattering Object

A homogeneous low-loss dielectric complex aircraft model.

Length Scale and Frequency Range

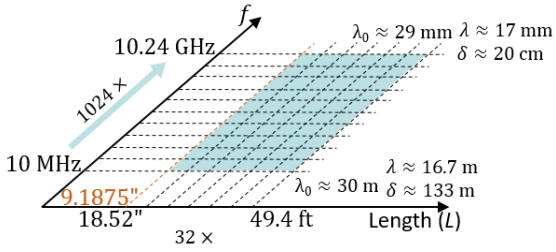

The problems of interest cover a range of ~64x in physical length scale and 1024x in frequency; the ranges are logarithmically sampled to yield 77 scattering problems. Because of the sampling distortions for the smallest aircraft, there are 77+1 unique scattering problems in Problem Set IVB. In these problems, the model sizes are in the range $0.007 \leq L/\lambda_0 \leq 514$ and $1.8 \times 10^{-3} \leq L/\delta \leq 76$, where λ_0 is the free-space wavelength and δ is the penetration depth of the resin.

Interesting Features

1. The logarithmic sampling is distorted along the size axis for the smallest model: the smallest Closed-Duct PRIME aircraft has L=9.1875'' (instead of L≈9.261''). The sampling is also distorted along the frequency axis: scattering from the smallest aircraft at frequencies $f \in$ {10, 20, 40, 80, 160, 320, 640, 1280, 2580, 5120, 7000, 10250} MHz are included in the problem set. These distortions are because of publicly available measurement data [1] and add 12 unique scattering problems to the set.

2. The model cannot be described sufficiently with a few equations, drawings, or pictures [1]; it presents modeling, meshing, and reproducibility challenges.

3. The low-loss dielectric material introduces extra uncertainties and sensitivities to RCS measurements and simulations [2].

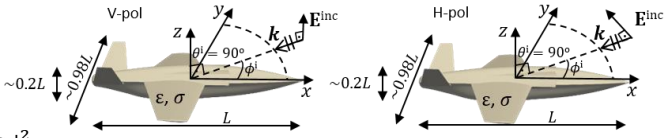

Quantities of Interest

Radar cross section (RCS) definition

$$\sigma_{vu}(\theta^{\mathrm{s}},\phi^{\mathrm{s}},\theta^{\mathrm{i}},\phi^{\mathrm{i}}) = \lim_{R\to\infty} 4\pi R \frac{\left|\hat{v}(\theta^{\mathrm{s}},\phi^{\mathrm{s}})\cdot\mathbf{E}^{\mathrm{scat}}(\theta^{\mathrm{s}},\phi^{\mathrm{s}})\right|^2}{\left|\hat{u}(\theta^{\mathrm{i}},\phi^{\mathrm{i}})\cdot\mathbf{E}^{\mathrm{scat}}(\theta^{\mathrm{i}},\phi^{\mathrm{i}})\right|^2} \quad : \text{RCS } (\mathrm{m}^2)$$

$$\sigma_{vu,\mathrm{dB}}(\theta^{\mathrm{s}},\phi^{\mathrm{s}},\theta^{\mathrm{i}},\phi^{\mathrm{i}}) = 10\log_{10}\sigma_{vu} \quad : \text{RCS in dB (dBsm)}$$

$$\sigma^{TH}_{vu,\mathrm{dB}}(\theta^{\mathrm{s}},\phi^{\mathrm{s}},\theta^{\mathrm{i}},\phi^{\mathrm{i}}) = \max\left(\sigma_{vu,\mathrm{dB}}, TH_{vu,\mathrm{dB}}\right) - TH_{vu,\mathrm{dB}} \quad : \text{Thresholded RCS}$$

1. Set $\theta^{\mathrm{i}} = 90^{\mathrm{o}}$. Vary $0^{\mathrm{o}} \leq \phi^{\mathrm{i}} \leq 180^{\mathrm{o}}$ (every 0.5^{o} in the interval).
2. Compute back-scattered $\sigma_{\theta\theta,\mathrm{dB}}$ and $\sigma_{\phi\phi,\mathrm{dB}}$ (the VV- and HH-pol RCS in dB) at $N_\phi = 361$ scattering directions.

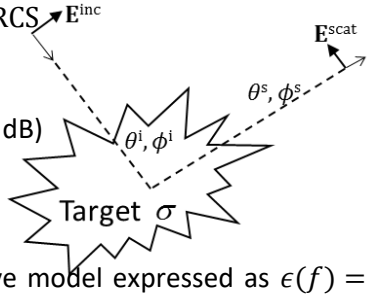

Material Properties

The permeability of the resin is the same as that of free space. A Debye model expressed as $\epsilon(f) = \epsilon_0\varepsilon_r(f)$, where

$$\varepsilon_r(f) = \varepsilon_r'(f) - j\varepsilon_r''(f) = 2.85 - j0.0687 + \frac{0.365 - j0.0602}{1 - jf(-0.1135 + j0.899)}$$

was used to calculate the complex permittivity of resin at the frequencies of interest. The reference simulation results were computed using precisely the permittivity values (i.e., to machine precision) shown in the below table. The above Debye model for the resin is slightly different than that in [2]. This is because a second set of measurements were performed following the submission of [2] that yielded slightly different values for the dielectric properties [3]. The average of the two measurements are used to fit the above Debye model as described in [3].

Frequency f (MHz)	ϵ'	ϵ''	Frequency f (MHz)	ϵ'	ϵ''
10	3.21	1.29×10^{-1}	2560	2.96	9.64×10^{-2}
20	3.21	1.29×10^{-1}	2580	2.96	9.63×10^{-2}
40	3.20	1.28×10^{-1}	5120	2.91	8.60×10^{-2}
80	3.19	1.28×10^{-1}	5125	2.91	8.60×10^{-2}
160	3.17	1.26×10^{-1}	7000	2.90	8.22×10^{-2}
320	3.13	1.23×10^{-1}	10 240	2.88	7.85×10^{-2}
640	3.08	1.18×10^{-1}	10 250	2.88	7.85×10^{-2}
1280	3.02	1.08×10^{-1}			

Performance Measures

Error Measure: Simulation errors shall be quantified using

$$avg.err_{uu,\mathrm{dB}}^{TH} = \frac{1}{2\pi}\int_0^{2\pi} \left|\sigma_{uu,\mathrm{dB}}^{TH}(\phi^s) - \sigma_{uu,\mathrm{dB}}^{\mathrm{ref},TH}(\phi^s)\right| d\phi^s \approx \frac{1}{N_\phi}\sum_{n=1}^{N_\phi} \left|\sigma_{uu,\mathrm{dB}}^{TH}(\phi_n^s) - \sigma_{uu,\mathrm{dB}}^{\mathrm{ref},TH}(\phi_n^s)\right| \ \ (\mathrm{dB}) \ \text{ for } u \in \{\theta,\phi\}$$

where

$$TH_{uu,\mathrm{dB}} = \max_{\phi^s} \sigma_{uu,\mathrm{dB}}^{\mathrm{ref}} - 80 \ (\mathrm{dB})$$

This error measure discounts errors in RCS values smaller than TH.

Cost Measure: Simulation costs shall be quantified using observed wall-clock time and peak memory/process

$$t^{\mathrm{wall}}(\mathrm{s}) \text{ and } mem^{\mathrm{maxproc}}(\mathrm{bytes})$$

as well as the "serialized" CPU time and total memory requirement

$$t^{\mathrm{total}} = N_{\mathrm{proc}} \times t^{\mathrm{wall}}(\mathrm{s}) \text{ and } mem^{\mathrm{max}} = N_{\mathrm{proc}} \times mem^{\mathrm{maxproc}} \ (\mathrm{bytes})$$

Here, N_{proc} denotes the number of processes used in a parallel simulation. It is expected that results will be reported for at least 2 runs: "Efficient" (small N_{proc}) and "Fast" (large N_{proc}).

Study 1: Error vs. Cost Sweep

Fix frequency and fix aircraft dimensions. Simulate many error levels (proxy: mesh densities) for 4 cases:
Case 1: f=10 MHz, L=9.1875 in Case 2: f=7 GHz, L=9.1875 in
Case 3: f=10 MHz, L≈49.4 ft (592.763 in) Case 4: f=320 MHz, L≈49.4 ft (592.763 in)
It's recommended to simulate as many error levels (mesh densities) as possible. 3-5 error levels is typical. A typical error-vs.-cost study will consist of 4x3-5=12-20 simulations.

Study 2: Frequency Sweep

Fix aircraft dimensions and error level (proxy: mesh density). Simulate many frequencies for 4 cases:
Case 1: L≈18.52 in, error level 1 (coarsest mesh) Case 2: L≈49.4 ft, error level 1 (coarsest mesh)
Case 3: L≈18.52 in, error level 2 (finer mesh) Case 4: L≈49.4 ft, error level 2 (finer mesh)
Frequencies shall be chosen as $f \in \{10, 20, 40, \ldots, 5120, 10240\}$ MHz. It's recommended to simulate as many frequencies as possible. A full frequency-sweep study will consist of 4x11=44 simulations.

Study 3: Size Sweep

Fix frequency and error level (proxy: mesh density). Simulate many sizes for 4 cases:
Case 1: f=10 MHz, error level 1 (coarsest mesh) Case 2: f=320 MHz, error level 1 (coarsest mesh)
Case 3: f=10 MHz, error level 2 (finer mesh) Case 4: f=320 MHz, error level 2 (finer mesh)
Dimensions shall be chosen as $L \in \{9.1875, 18.524, 37.04, \ldots, 296.3815, 592.763\}$ in. It's recommended to simulate as many sizes as possible. A full size-sweep study will consist of 4x7=28 simulations.

Reference Quantities of Interest

The following RCS data are made available in the benchmark to enable participants to calibrate their simulators:

4 RCS measurement results corresponding to the smallest aircraft (L=9.1875 in) at frequencies $f \in$ {2580, 5120, 7000, 10250} MHz. These measurements were made using an aircraft scale model of size L=9.1875 in. These data are provided for ϕ^{i} sampled every 0.25^{o}.

4 RCS simulation results for the smallest aircraft at the above 4 frequencies found by using the ARCHIE-AIM code, a frequency-domain FFT-accelerated integral-equation solver developed at UT Austin [4]-[6].

References

[1] J. T. Kelley, A. Maicke, D. A. Chamulak, C. C. Courtney, and A. E. Yılmaz, "Adding a reproducible airplane model to the Austin RCS Benchmark Suite," in *Proc. Applied Comp. Electromagnetics Society (ACES) Symp.*, July 2020.

[2] J. T. Kelley, A. E. Yilmaz, D. A. Chamulak, and C. C. Courtney, "Measurements of non-metallic targets for the Austin RCS benchmark suite," in *Proc. Ant. Meas. Tech. Assoc. (AMTA) Symp.*, Oct. 2019.

[3] J. T. Kelley, D. A. Chamulak, C. C. Courtney, and A. E. Yilmaz, "Measurements of non-metallic targets for the Austin RCS benchmark suite," *presentation in AMTA Symp.,* Oct. 2019. Available: https://github.com/UTAustinCEMGroup/AustinCEMBenchmarks/Austin-RCS-Benchmarks/AMTA2019presentation.pdf

[4] M. F. Wu, G. Kaur, and A. E. Yılmaz, "A multiple-grid adaptive integral method for multi-region problems," *IEEE Trans. Antennas Propag.*, vol. 58, no. 5, pp. 1601-1613, May 2010.

[5] F. Wei and A. E. Yılmaz, "A more scalable and efficient parallelization of the adaptive integral method part I: algorithm," *IEEE Trans. Antennas Propag.*, vol. 62, no. 2, pp. 714-726, Feb. 2014.

[6] J. W. Massey, V. Subramanian, C. Liu, and A. E. Yılmaz, "Analyzing UHF band antennas near humans with a fast integral-equation method," in *Proc. EUCAP*, Apr. 2016.